

Verification of Sciamachy's Reflectance over the Sahara

J.R. Acarreta and P. Stammes

*Royal Netherlands Meteorological Institute
P.O. Box 201, 3730 AE de Bilt, The Netherlands
Email Address: acarreta@knmi.nl, stammes@knmi.nl*

ABSTRACT

We present a preliminary report on the verification of the Sciamachy L1c data (geolocated and calibrated L1b data) for a clear state over the Sahara. Auxiliary SeaWifs, MODIS and PMD images are used to verify the absence of clouds. The available L1b Sciamachy radiance and irradiance are calibrated with the tool SciaL1C (version 2.0.7), dumping the data in ASCII format with the tool Pds2Ascii (version 2.0.7). The spectral absorption bands due to O₃, H₂O, CH₄, etc. are clearly identified. It is found that unexpected spectral spikes are seen in the Solar Irradiance product. Some inconsistencies between the measured reflectance and radiative transfer simulations are also detected in channels 1 to 6.

1. Selection of the State

The determination of the quality of the SCIAMACHY reflectance can be done more easily if the region under consideration does not contain clouds. Moreover, a constant ground albedo is desired. Although observations over the ocean can be considered, we selected one state over the Sahara. The state-of-the-art calibrated L1b data (recalibrated orbit 2509 of August, 23 2002, delivered to us in November 2002) is used as input for the tool SciaL1C. That tool is called with the default options "--cal 0,1,2,3,4,5,7 -cat 1 -nadircluster".

The verification presented in this work was done twice, one with the polarization correction switched off and one with the correction switched on. The radiances were virtually the same in both cases, except for the expected change in the region 340-360 nm. Due to the current uncertainties of this correction (see the work of [2] in this volume) all the results are presented with the correction switched off, except if it is stated otherwise.

In order to select a clear state (i.e., without clouds), we use auxiliary MODIS and Seawifs images (Fig. 1). We do, also, a comparison (not shown) of the reflectance for the clusters 9 (392-320nm) - 26 (754-776 nm) to see if the reflectance of all the observations, within each orbital state, is reasonably homogeneous. This test includes the assumption that the cloud coverage is not equal to unity in any state near the Sahara region. Hence, states with a non-homogeneous reflectance are discarded. The information from the PMDs shown in Fig. 1 (see [3] for details) confirms the clear state over the Northern Sahara (marked with a yellow arrow in Fig. 1).

2. Solar Irradiance data product of orbit 2509

The solar irradiance that is included in the Sciamachy data product (known as the GADS Mean Reference Spectrum; see [1]) is shown in Fig. 2. It is clear that the overlapping regions (for instance at ≈ 600 or ≈ 1000 nm) do not show a smooth transition, and that some spikes are present in different channels, with a clear increase in their number in the last part of channel 6 (longest wavelengths). The order of magnitude of the calibrated irradiance (about $1 \text{ Watt} / \text{nm} / \text{m}^2$) and global shape (\approx black body) is fully compatible with the values available through the literature.

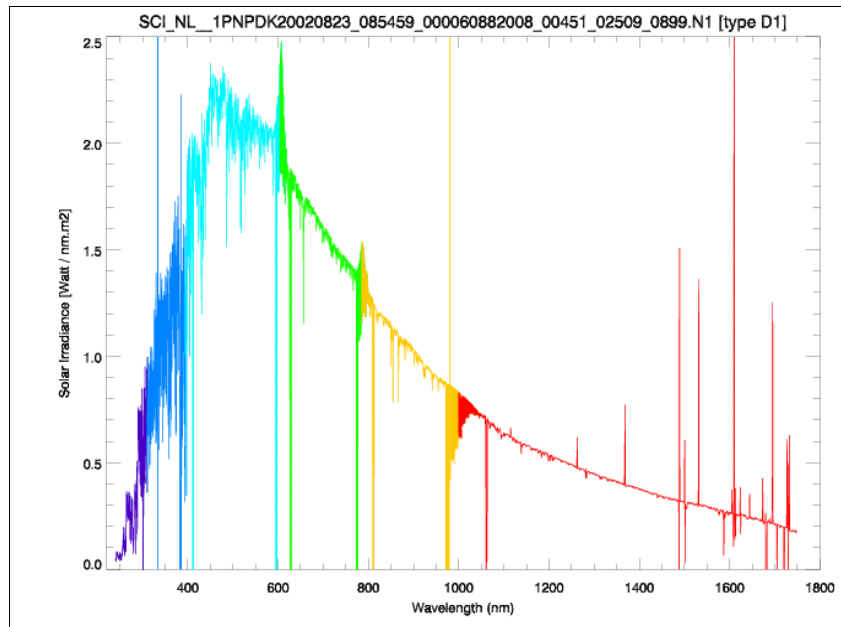


Fig. 2: Mean Reference Spectrum for the orbit 2509.

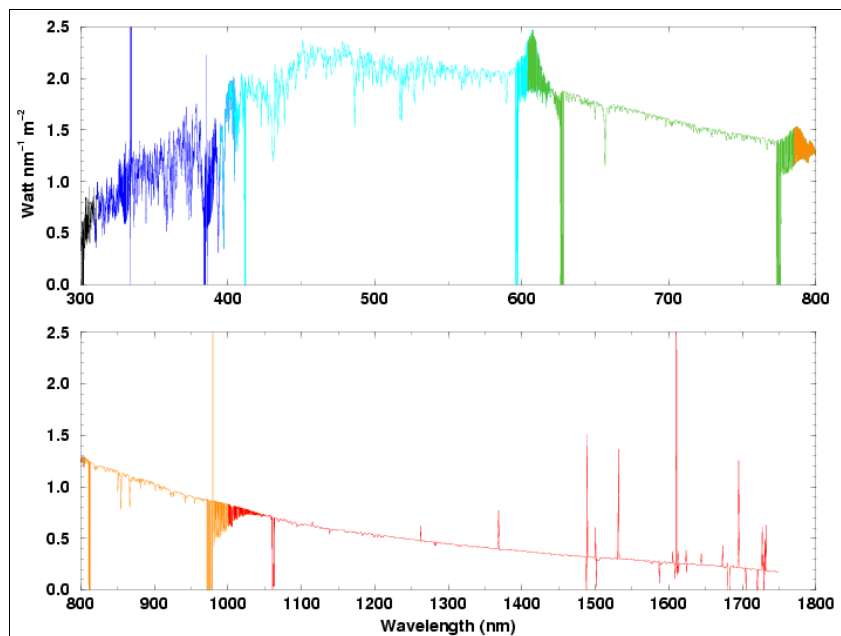


Fig. 3: A more detailed view of Fig. 2

3. Earth Reflectance

As an example of the spectral capabilities of Sciamachy, Fig. 4 shows the reflectance spectrum as the median value of all the reflectances within the selected state. The reflectance of each observation is calculated as the ratio of the radiance over the irradiance, multiplied by π and divided by the $\text{Cos}[\text{SolarZenithAngle}]$ (all those values are extracted from the L1c file; see [1] for details). Fig. 4 shows with labels the most representative absorptions due to O_3 , H_2O , etc. Some spurious signals appear near the transition between channels. Note that the calculation of the reflectance needs to interpolate the irradiance to the wavelength grid of the radiance. This process should, in principle, be able to transform the radiance into reflectance without any artefact, although only if the irradiance is always a smooth function with the wavelength.

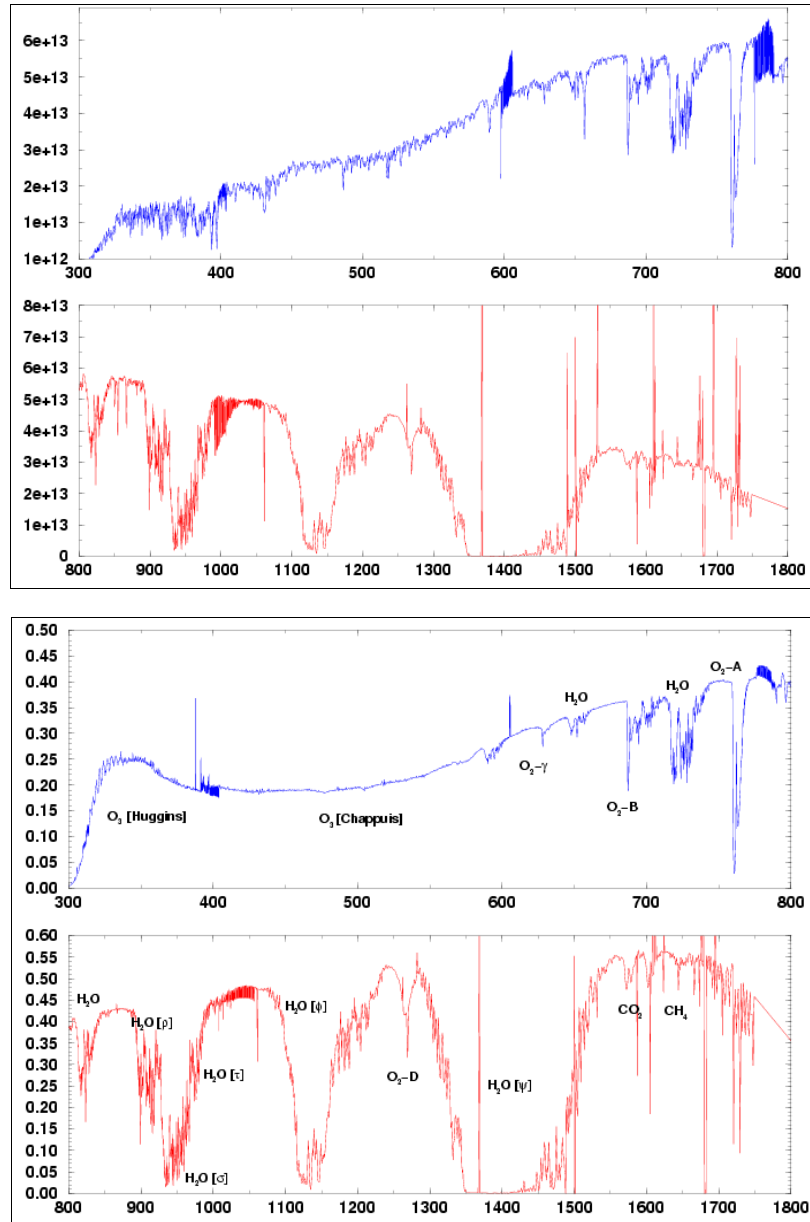


Fig. 4: Median radiance (upper) and reflectance (lower) vs. wavelength (nm) for the selected state. The radiance has units of photons per $\text{cm}^2/\text{sr}/\text{nm}$.

4. Comparison with Simulations

The observations within the selected state are selected and averaged to an East (E), Central East (CE), Central West (CW) and West (W) “big” ground pixel (middle image of Fig. 1; see also Fig. 5). The comparison with the simulations (Fig. 7, Fig. 8, Fig. 9, Fig. 10) corresponds to the subset of clusters 5 (304-314 nm) – 31 (790-798 nm).

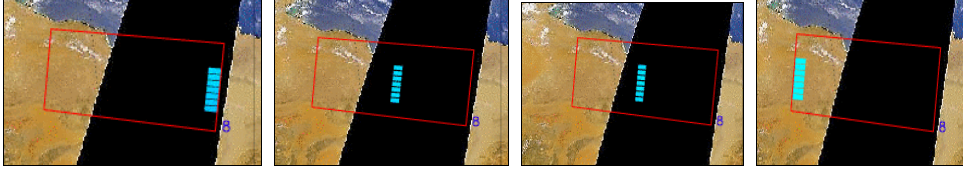


Fig. 5: Definition of the "big" ground pixels E, CE, CW and W (from left to right).

The selected (5-31) Sciamachy clusters have a ground pixel size of $\approx 30 \times 60 \text{ km}^2$ (along \times across track). The new “big” pixels are $\approx 210 \times 60 \text{ km}^2$. The reflectance of each big pixel is compared with simulations produced by the radiative transfer code DAK (Doubling-Adding KNMI [4], [5]) including the ground albedo spectrum from [6] (see also Fig. 6). The comparison is done with and without the polarization correction (Fig. 7, Fig. 8, Fig. 9, Fig. 10). The calculations assume a mid-latitude summer profile scaled to the observed ground pressure, a vertical ozone column of 275 DU and no other trace gases or aerosols. Polarization is included. The geometry for the simulations (solar zenith angle, viewing zenith angle and relative azimuth) corresponds to the mean value of all the observations of the “big” ground pixels (defined in Fig. 5).

The simulations show that for both East and West pixels, there is no good agreement between the observations and the simulations. The West pixel (Fig. 10) has a better behaviour than the East pixel (Fig. 7). The differences are not systematic, in the sense that they cannot be explained by a constant shift for all the wavelengths. Note that the polarization correction does not improve the situation, because its largest effect is limited to the region $\approx 350 \text{ nm}$. The maximum difference, up to 30%, is found in the channel 4, although only for the East pixel. It is also clear that in the UV, the reflectance is about 20% too low for all the pixels. On the other hand, the West pixel shows a better agreement, with a maximum $\approx 20\%$ difference only in the channel 2. Note that the climatology for the surface albedo from [6] (shown in Fig. 6) might not be sufficiently representative, due to the surface variability within the selected state. This would not appreciably change the UV reflectance, but could change the VIS ($\approx 550 \text{ nm}$) and NIR ($\approx 800 \text{ nm}$) reflectance.

5. Conclusions

We have presented the reflectance measured by Sciamachy for a state over the Sahara. Using auxiliary information, the state has been accepted as a good example of a cloud free region. From a global point of view, the reflectance shows a good behaviour, containing the expected gas absorption features within the range 300 – 1800 nm. However, some spikes are identified. Their origin is unknown, although probably they are related to bad elements of the Sciamachy detectors. The official tool Enviview (version 2.0.7) shows also that the spikes seen in Fig. 2 are not artefacts introduced by the tools SciaL1c or Pds2Ascii. More work is needed to verify the quality of the solar irradiance product. Comparison with other sources, as for example SOLSPEC, would give a better characterization of the accuracy of the solar irradiance.

The observations are compared with radiative transfer calculations, showing that differences up to 30% are present, with a clear underestimation in the UV region. From the set of observations it can be concluded that the polarization correction has negligible effects outside the interval 340-360 nm. The expected absorption bands due to absorbers like O_3 or H_2O are clearly seen within the range 300-1800 nm.

6. References

1. *Sciamachy Level 0 to 1c Processing: Algorithm Theoretical Basis Document* (or ATBD), ENV-ATB-DLR-SCIA-0041, DLR (version December 14, 2000).
2. Tilstra *et al.* (these proceedings)
3. De Graaf *et al.* (these proceedings)
4. De Haan, J.F., Bosma, P.B., Hovenier, J.W., *The Adding Method for Multiple Scattering Calculations of Polarized Light*, *Astron. & Astrophys.*, 183, 371-393, 1987
5. Stammes, P., *Spectral Radiance Modeling in the UV-Visible Range*, IRS2000, Current Problems in Atmospheric Radiation, eds. W.L. Smith, Y.M. Timofeyev, A. Deepak Publ., Hampton (VA), pp 385-388, 2001.
6. Koelemeijer, R., de Haan, J.F., Stammes, P., *A Database of Spectral Surface Reflectivity in the Range 335-772 nm Derived from 5.5 Years of GOME Observations*, JGR, 2002 (in press).

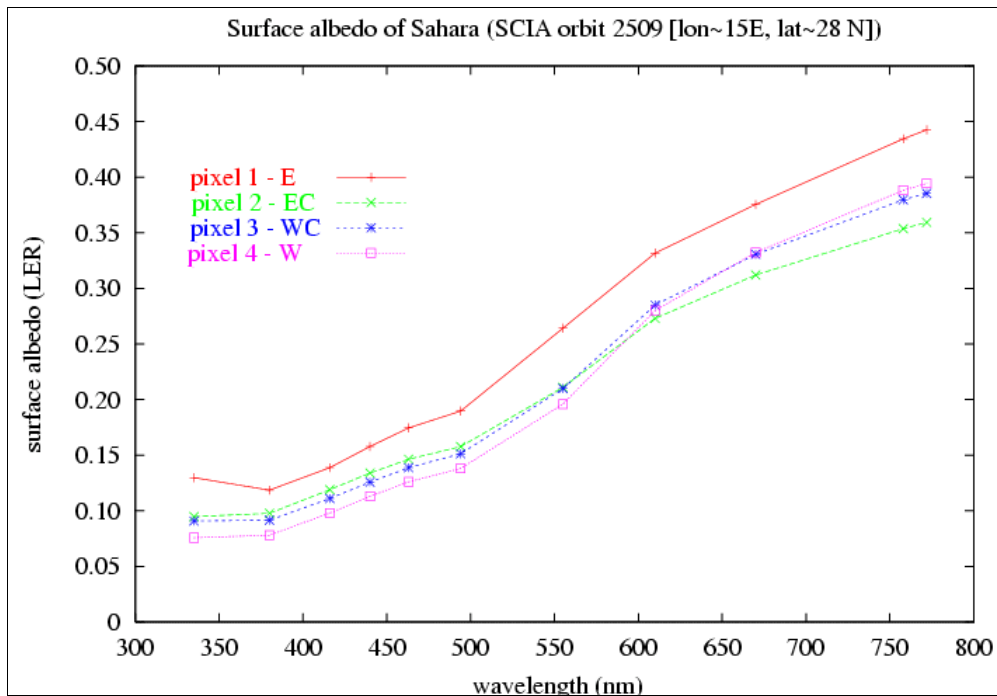


Fig. 6: Assumed surface albedo for the Sahara desert (from [6])

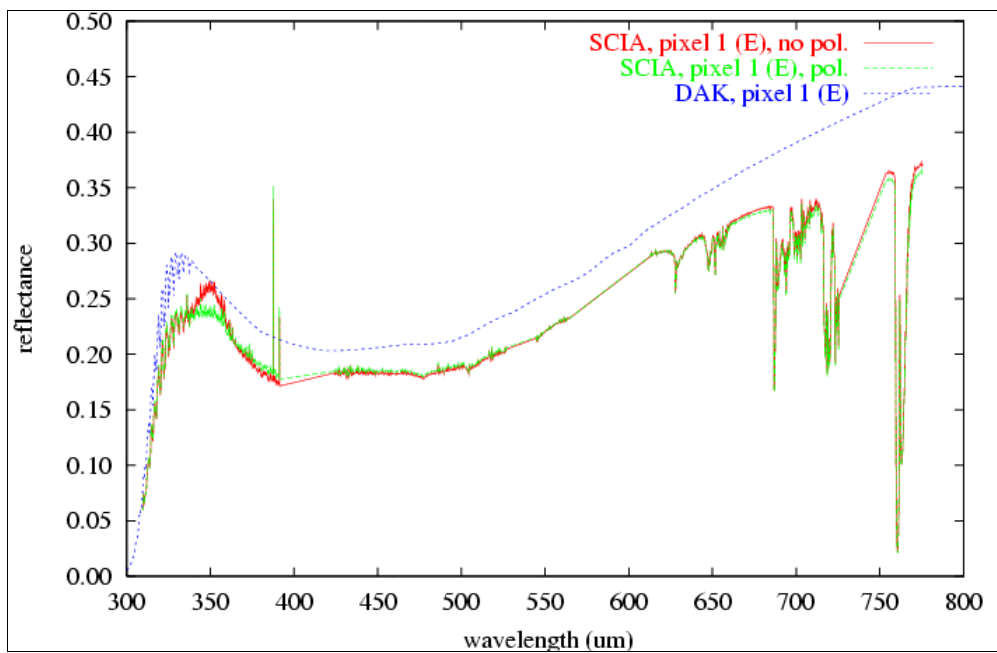


Fig. 7: Comparison with simulations (East pixel; see Fig. 5).

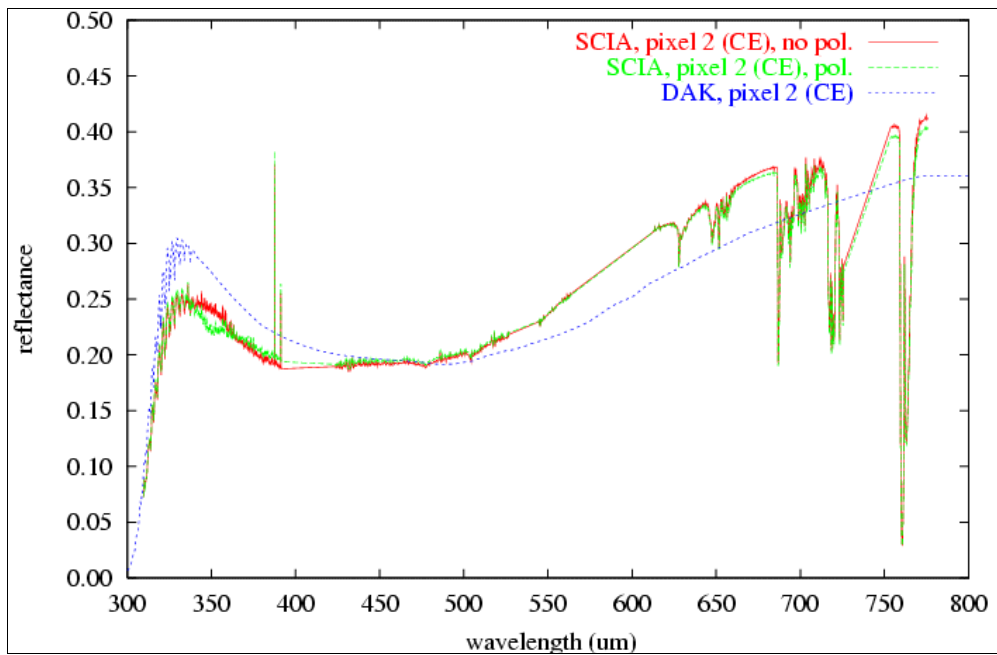


Fig. 8: Comparison with simulations (Central East pixel; see Fig. 5).

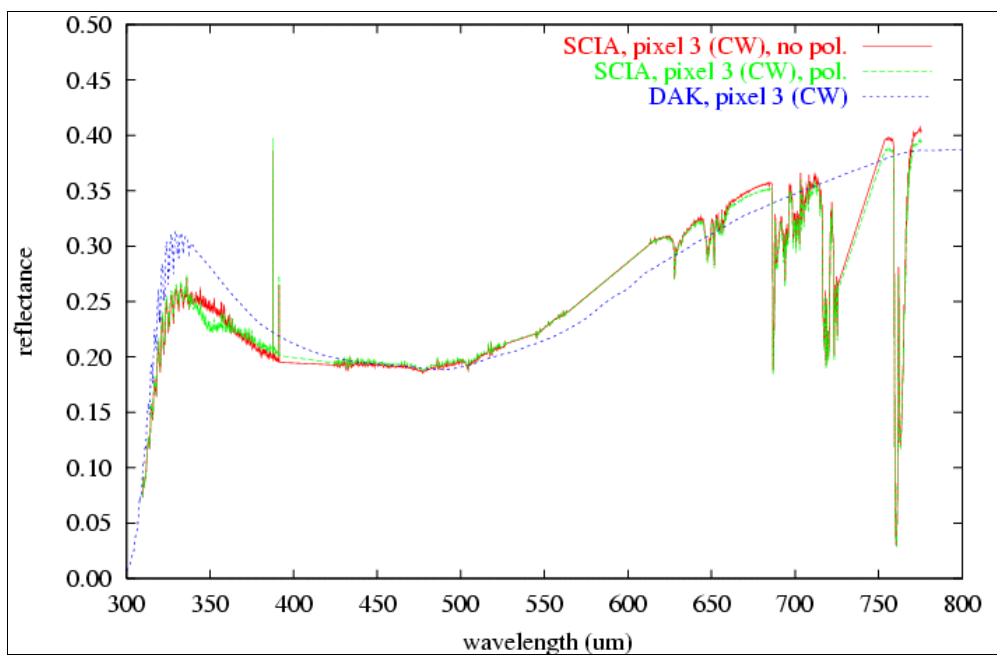


Fig. 9: Comparison with simulations (Central West pixel; see Fig. 5).

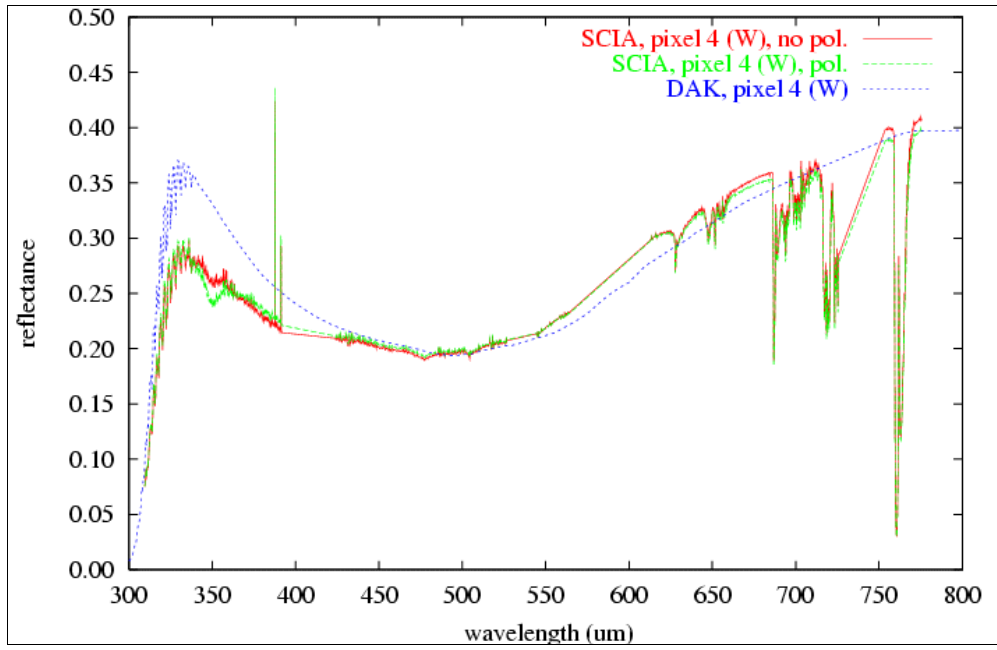


Fig. 10: Comparison with simulations (West pixel; see Fig. 5).